Electric-field-induced reorientation and flip in domain magnetization and light diffraction in an yttrium-iron-garnet/lead-zirconate-titanate bilayer

I. V. Zavislyak, V. P. Sohatsky, M. A. Popov, and G. Srinivasan

Phys. Rev. B **87**, 134417 — Published 22 April 2013

DOI: 10.1103/PhysRevB.87.134417

Electric field induced reorientation and flip in domain magnetization and light diffraction in an yttrium iron garnet-lead zirconate titanate bilayer

I.V.Zavislyak,[1] V.P.Sohatsky,[1] M.A.Popov,[1] and G.Srinivasan[2]

[1] Radiophysics Department, Taras Shevchenko National University of Kyiv, Kyiv, 01601, Ukraine

[2] Physics Department, Oakland University, Rochester, MI 48309

Abstract

A continuous reorientation and an abrupt flip to a canted structure in the magnetization of stripe domains are observed under the influence of an electric field in an yttrium iron garnet (YIG) – lead zirconate titanate (PZT) bilayer. Magneto-optic techniques have been utilized for the observation of the domain structure and the magnetization-flip. It is found that electrically generated mechanical stress in PZT induces an uniaxial anisotropy field in YIG which is large enough to initially cause a gradual change in the domain magnetization and then a transition from out-of-plane orientation to a canted state for a threshold electric field. Additional evidence for the spin-flip has been obtained from data on the modulation of intensity of linearly polarized light due to diffraction by the stripe domains. A comprehensive theory for the voltage-induced magnetization-flip is discussed and compared with the data. The magnetic transitions and the theory discussed here are of interests for electric field controlled magneto-optic and spintronic devices.

I. Introduction

Spin-flip transitions associated with magnetic ordering in materials that are initiated by an external static magnetic field or temperature dependence of anisotropy fields are well known [1-3]. Meanwhile there is another potential path for studies on such transitions: electric-field induced modification of uniaxial anisotropy field in multiferroic composite materials [4-9]. The most promising multiferroics for such studies are magnetoelectric (ME) composites made by combining ferroelectric and ferro- or ferrimagnetic substances in which the ME response is orders of magnitude stronger than in single-phase ME materials at room temperature [6]. The ME effect in the mechanically bound two-phase composite materials is a product-property arising from the magnetostriction and piezoelectric effects. In a ferrite-ferroelectric composite, for example, the static magnetization and high frequency electromagnetic properties can potentially be controlled with an applied voltage [4-14]. Several recent studies reported experiments on electric field induced magnetization changes in ferromagnetic-piezoelectric ME systems, including magnetization reversal in ferrimagnetic nano-pillars, magnetization rotation in Ni nano-rings and nano-bars, and changes in the magnetic anisotropy and stripe domain pattern modifications in Ni thin films [10-14].

Bilayers of yttrium iron garnet, $Y_3Fe_5O_{12}$ (YIG), and lead zirconate titanate (PZT) have been used extensively in the past for studies on the converse ME effects, i.e., voltage control of magnetic parameters in YIG [6-9]. Studies of significance in this regard include voltage tuning of M vs H, ferromagnetic resonance, and magneto-acoustic resonance [6-9]. A strong converse ME effect in YIG-PZT was inferred from these studies. A variety of novel voltage tunable ferrite devices including microwave resonators, filters, phase shifters, and delay lines were demonstrated with the use of YIG-PZT [6-9].

This work is on the optical observation and theory of magnetization-flip due to an applied electric field in composites with single crystal thin films of YIG and polycrystalline PZT. Films of YIG in general are grown by the liquid phase epitaxy on gadolinium gallium garnet (GGG)

substrates. Such films show an uniaxial anisotropy field, resulting in a stripe domain structure. LPE grown YIG films are of particular interests due to excellent high-frequency magnetic properties [15, 16]. Thin films are transparent in the visible region of the EM spectrum and show a large Faraday effect [17]. Magneto-optic techniques have been used in this study for the observation of (i) 180^0 magnetic stripe domains with out-of-plane magnetization M_z in YIG and (ii) diffraction of light by the stripe domains when an electric field E is applied to PZT. With the application of a DC voltage V across PZT, a gradual decrease in M_z is observed with increasing V until a threshold voltage V_t when a first -order phase transition takes place with an abrupt change in the magnetization vector $\vec{M}$ to a canted state. The flip in the domain magnetization is a macroscopic analog of the well-known spin-flip phase transitions in ferrimagnetic and antiferromagnetic materials and is characterized by a step-wise rotation of $\vec{M}$ in individual domains instead of sublattices. For $V > V_t$, the canting angle shows a gradual increase and a corresponding decrease in M_z. The changes in the domain magnetization are due to an E-induced uniaxial anisotropy in YIG that arises from piezoelectric deformation in PZT. A model for the effects has been developed and theoretical estimates are in good agreement with the data.

This paper is organized as follows. Section II provides a theoretical description of voltage-controlled magnetic reorientation and spin-flip processes. Expressions are obtained for the stress-induced anisotropy fields and the free energy density for the domain structure that depends on anisotropy fields. In Section III we discuss the choice of specific ferrite/piezoelectric metamaterial and details on the experimental setup. Section IV present the experimental results on the voltage-induced reorientation and flip in magnetization vectors in the stripe domains. Also, results on polarized light diffraction by the stripe domain structure are presented and the possibility of voltage control of transmitted light intensity and modulation is demonstrated and discussed. Section V provides a summary and conclusion.

II. Theory of electric-field control of domain magnetization

a. Stripe domains and free energy

We consider an YIG film with stripe domains as in Fig.1. The external static magnetic field H_0 is in the film plane and directed along $[1\bar{1}0]$ axis. The surface normal is along [111], and with $[11\bar{2}]$ direction completes the right-handed orthogonal coordinate system (Fig.1). The domain walls are parallel to H_0 and perpendicular to the sample surface. Such a model is fully consistent with the domain structure observed in our experiment (as discussed in details later). The orientation of $\vec{M}$ in each domain (labeled M_1 and M_2) is specified by the respective azimuth and polar angles (φ_i, θ_i) in spherical coordinate system whose polar axis coincides with the sample normal and the azimuth angle is measured from the $[11\bar{2}]$ direction. The equilibrium direction for the domain magnetization is determined by minimizing the free energy. Assuming the stripe domain structure to be periodic in the $[1\bar{1}2]$ direction, we estimate the free energy per unit volume as [18-22]

$$W = W_{an} + W_Z + W_{dd} + W_{dw}$$

where W_{an} is the crystalline anisotropy energy [15], W_Z is the Zeeman energy, W_{dd} is the magnetic dipole-dipole energy that includes demagnetization energy for the net M of the sample and demagnetization energy of domain walls, and W_{dw} is the domain wall energy.

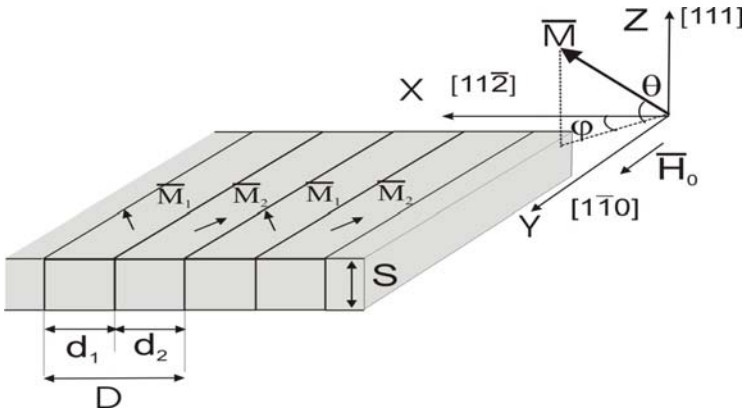

Fig. 1. Diagram showing the stripe domain structure in yttrium iron garnet film and magnetic field and magnetization directions assumed in the theory.

The expression for free energy density for the stripe domain structure is given by

$$W/M_0 = \nu_1 H_{cub}(\frac{1}{4}\cos^4\theta_1 + \frac{1}{3}\sin^4\theta_1 - \frac{\sqrt{2}}{3}\sin\theta_1\cos^3\theta_1\sin 3\varphi_1) - \nu_1\frac{H_{U1}}{2}\sin^2\theta_1 - \nu_1\frac{H_{U2}}{4}\sin^4\theta_1 -$$
$$-\nu_1 H_0\cos\theta_1\sin\varphi_1 + \nu_2 H_{cub}(\frac{1}{4}\cos^4\theta_2 + \frac{1}{3}\sin^4\theta_2 - \frac{\sqrt{2}}{3}\sin\theta_2\cos^3\theta_2\sin 3\varphi_2) -$$
$$-\nu_2\frac{H_{U1}}{2}\sin^2\theta_2 - \nu_2\frac{H_{U2}}{4}\sin^4\theta_2 - \nu_2 H_0\cos\theta_2\sin\varphi_2 + 2\pi N_\perp M_0(\nu_1\sin\theta_1 + \nu_2\sin\theta_2)^2 + \quad (1)$$
$$+2\pi N_\parallel M_0(\nu_1\cos\theta_1\sin\varphi_1 + \nu_2\cos\theta_2\sin\varphi_2)^2 + 2\pi N_{dw}\nu_1\nu_2 M_0(\cos\theta_1\cos\varphi_1 - \cos\theta_2\cos\varphi_2)^2$$
$$+\frac{D}{S}\frac{M_0}{\pi^2}(\sin\theta_1 - \sin\theta_2)^2\sum_{n=1}\frac{1}{n^3}(1-\cos 2\pi n\nu_1) + \frac{2\gamma_{dw}}{M_0 D}$$

where $H_{cub} = \frac{K_{cub}}{M_0}$ is the cubic anisotropy field (note that for YIG: $K_{cub} < 0$ and H_{cub}=-45 Oe), $H_{U1} = \frac{2K_{U1}}{M_0}$, $H_{U2} = \frac{4K_{U2}}{M_0}$ are the first and second order uniaxial anisotropy fields, respectively, M_0 is the saturation magnetization (M_0=140 G), $\gamma_{dw} = \gamma_{dw}(\varphi_i, \theta_i, K_{U1}, K_{U2}, K_{cub}, D_{ex})$ is the specific wall energy [21], $N_\perp$ is the demagnetization factor in the perpendicular-to-plane direction ($N_\perp \approx 1$), $N_\parallel$ is the in-plane demagnetizing factor in the direction parallel to H_0 ($N_\parallel << 1$), $N_{dw} \approx S/(D+S)$ is the domain wall demagnetization factor [22], and $\nu_i = d_i/D$ is the volume of each part of the domain (in all of our calculations the stripe domains are assumed to be equal in volume $\nu_1 = \nu_1 = 1/2$). The equilibrium state can be obtained by minimizing W with respect to the parameters $\theta_1, \varphi_1, \theta_2, \varphi_2$ for specific values of H_0 and H_{U1} and H_{U2}. Note that the last two terms in Eq.(1) include the domain period D and these terms define the equilibrium domain width D_0. Indeed while demagnetizing energy tends to make domains infinitely small, the accompanying increase in domain wall energy prevents this, thereby stabilizing the domain period at some optimum value [21]. We will concentrate our attention on the region where the domain period remains constant.

It is important here to discuss conditions under which the above model is valid. Obviously, the theory is applicable only when the domain structure corresponds to the structure

in Fig.1. As we have found out during experiments (discussed in Section III), for H_0 less than approximately 2 Oe, the periodic stripe domain is transformed into labyrinth structure with the domains along three equivalent <110> directions in the film plane, with C_3 rotational symmetry about the [111] axis (see Fig. 5 a). This lower boundary is defined by the energy barrier between adjacent <110> directions, namely energy difference between <110> and <112> axes. On the high field side, when H_0 exceeds approximately 8 Oe, domains become substantially unequal in width, with energetically favorable one prevailing. This can also be observed by the appearance of the even maxima in the diffraction pattern (Fig. 5 c) as discussed later. We can set the high field limit according to d_2/d_1>1.1, assuming d_2 is for the energetically favorable domain.

b. Theory of electric field induced anisotropy

Next we consider magnetoelastic energy of YIG film grown on GGG. The energy is a function of strain tensor ε_{ij}, direction cosines of magnetization α_i, and direction cosines of the normal to the substrate β_i [23]. The exact form of this phenomenological expression is determined by the crystal symmetry. It was found that for ferrites with cubic symmetry grown on (111) substrate ($\beta_i = 1/\sqrt{3}$), energy could be represented as [24]

$$W_{me} = -K_{U1}\alpha_z^2 + K_{cub}(\alpha_1^2\alpha_2^2 + \alpha_2^2\alpha_3^2 + \alpha_1^2\alpha_3^2) - K_{U2}\alpha_z^4 \qquad (2)$$

where $K_{U1} = 3b_2\varepsilon_a - 3b_4\varepsilon - \frac{3}{2}b_5\varepsilon_a$, $K_{U2} = \frac{9}{4}b_5\varepsilon_a$, $K_{cub} = 3(b_3 + \frac{2}{3}b_4)\varepsilon - b_5\varepsilon_a$, $\varepsilon_a = \frac{\sigma}{3c_{44}}$,

$\varepsilon = \frac{\sigma}{c_{11}-c_{12}}\left(\frac{1}{3} - \frac{c_{12}}{c_{11}+2c_{12}}\right)$, α_z is a direction cosine with respect to the <111> axis, c_{ij} being YIG stiffness constants, b_i is the magnetoelastic coupling coefficients, and σ is the mechanical stress applied along the surface normal. Equation (2) has the classical form of mixed (cubic and uniaxial) magnetocrystalline anisotropy energy and hence the coefficients $K_{U1}(\sigma)$, $K_{U2}(\sigma)$, and $K_{cub}(\sigma)$ have physical meaning of the stress-induced anisotropy constants (first and second

order uniaxial and first order cubic, respectively) [15]. Consequently, magnetocrystalline anisotropy energy constants and fields in YIG films should be treated as comprising of two parts, for instance, $H_{U1}^{\Sigma} = H_{U1}^{G} + H_{U1}^{E}(\sigma)$, where H_{U1}^{G} is the growth induced anisotropy [23]. The origin of the perpendicular magnetic anisotropy is growth induced strain at the film-substrate interface and arises due to two factors: (i) slight mismatch in the lattice constants of the GGG substrate and the YIG film, and (ii) the difference in the thermal expansion coefficients of GGG and YIG. The term $H_{U1}^{E}(\sigma)$ is due to the (*E*-field)-induced piezoelectric strain term. Assuming $b_3, b_4, b_5 << b_1, b_2$, we can neglect $K_{U2}^{E}(\sigma)$ and $K_{cub1}^{E}(\sigma)$ and obtain the well-known expression [25-27]

$$K_{U1}^{E}(\sigma) = \frac{b_2 \sigma}{c_{44}} = -\frac{3}{2}\lambda_{111}\sigma \qquad (3),$$

where $\lambda_{111} = -\frac{2b_2}{3c_{44}}$ is the magnetostriction constant[28].

In the case of a YIG-PZT composite structure, voltage-induced mechanical stress in YIG could be expressed as $\sigma = \frac{E}{1-\nu}\frac{V}{S}d_{31}$, where E is Young's modulus ($E = 2 \cdot 10^{11}$ Pa for YIG [28]), ν is the Poisson's ratio ($\nu = 0.29$), $d_{31} = -2.7 \cdot 10^{-10}$ m/V is the piezoelectric coefficient for PZT, *V* is the applied voltage, and *S* is the PZT thickness. Therefore, we obtain

$$H_{U1}^{E}(V) = \frac{2K_{U1}}{M_S} = -\frac{3E}{1-\nu}\frac{\lambda_{111}}{M_S}\frac{d_{31}}{S}V \quad . \qquad (4)$$

Hence, the magnetoelectric effect in layered ferrite-piezoelectric structure manifests as voltage-induced generation of the first order unaxial anisotropy field in the ferrite film [5]. Since the electric field induces piezoelectric strain in PZT that is transferred to YIG and GGG, the overall uniaxial anisotropy field in YIG will depend critically on the thickness of both the YIG and GGG. For a given E-value one anticipates a decrease in the anisotropy field with increasing YIG film thickness.

c. Voltage controlled magnetization-flip

Minimization of the energy density [Eq.(1)] revealed the presence of three different local energy minima, namely, the out-of-plane state (OOP, $\theta_1 \approx \pi/2, \theta_2 \approx -\pi/2$), the in-plane state (IP, $\theta_1 \approx 0, \theta_2 \approx 0$) and the canted state ($\theta_1 \approx \theta_c, \theta_2 \approx -\theta_c$, $0 < \theta_c < \pi/2$ and θ_c depends on H_0 and H_{U1} values).

In order to determine the influence of the uniaxial anisotropy field on equilibrium domain structure, we calculated the dependence of energy of these three states on H_{U1} for M = 140 G, H_{cubic} = -45 Oe, and H_0 =4 Oe. We assumed the second order anisotropy field $H_{U2} = -H_{U1}/3$ [29]. Note that H_{U1} should be treated as a total uniaxial anisotropy field, consisting of growth induced H_{U1}^G and electric field-induced $H_{U1}^E(V)$ parts. The domain energy is plotted as a function of H_{U1} in Fig.2. It is seen in Fig. 2 that for positive uniaxial field the domain magnetization is oriented predominantly along the surface normal (OOP state), while with decreasing H_{U1} the magnetization experiences a transition to a canted configuration. In this phase θ_c changes from 17^0 to 23^0 for H_{U1} from -10 Oe to 10 Oe and the out-of-plane component of magnetization $M_{1,2}^z = \left| M_0 \sin\theta_{1,2} \right|$ is in the range 41-55 G. The perpendicular magnetization is of specific interest because it is the component that determines the Faraday rotation and, thus, is detected in our magneto-optic experiments. Since the regions of stability of magnetic phases under consideration overlap, this is a first-order magnetization-flip phase transition [1]. It is demonstrated in Fig.3 where the energy for perpendicular-to-plane magnetization state is depicted as a function of applied voltage. Here $H_{U1}^E(V)$ was calculated using Eq.(4) and the measured material parameters. In order to account for ferroelectric hysteresis in PZT, we have expanded the phase transition point into a finite-width region. Previous microwave experiments facilitated direct measurements of $H_{U1}^E(V)$ hysteresis showing an average width of roughly 30 V [5]. That value was transferred onto the hysteresis region in Fig. 3.

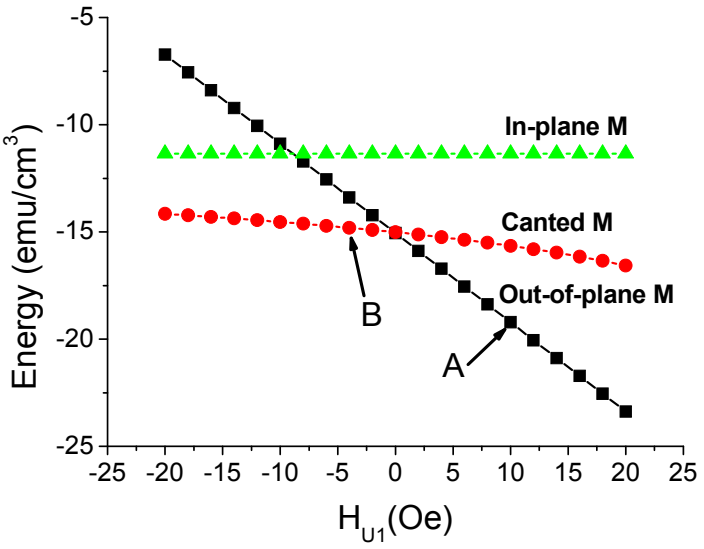

Fig. 2. Equilibrium energy of domain magnetization states, i.e., out-of-plane, in-plane and canted states, as a function of uniaxial anisotropy field. A and B correspond to regions of antiparallel and canted domain magnetization states (as in Fig 3).

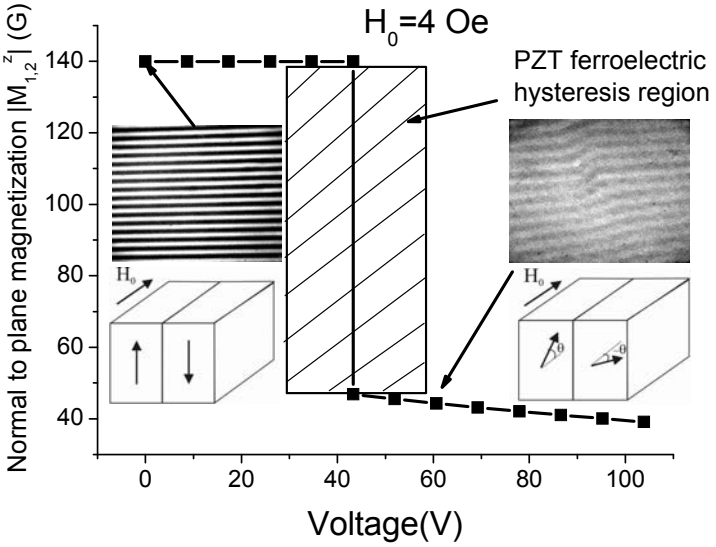

Fig. 3. Out-of-plane component of equilibrium magnetization vs. applied voltage. H_{U1}^{G} is assumed to be 10 Oe. Magnetooptical images of domain structure before and after magnetization-flip to canted structure are also shown.

To summarize, if the initial growth induced uniaxial anisotropy of magnetic film is rather small ($|H_{U1}| < 10$ Oe), one can cause drastic modification of the equilibrium magnetization orientation with the application of a voltage (and a stress-induced uniaxial anisotropy field). Thus, the possibility for substantial electric field control of magnetic domain structure arises.

III. Experiment

The experimental set up for the observation of the domain structure and corresponding diffraction pattern in polarized light is presented in Fig.4. The intensity of the diffracted light and the Faraday rotation of non-diffracted light were measured with a photodetector for quantitative characterization of the domain structure transformation. In this experiment, YIG film was bonded to PZT disk of diameter 10 mm and thickness 0.2 mm. The PZT disk had silver electrodes, was poled by heating to 320 K and cooling in E=20 kV/cm. A 2 mm diameter hole was drilled in the disk to provide transmission of light. YIG films 10 μm in thickness on 0.5 mm thick GGG substrates were used. As mentioned earlier in Sec.I, the YIG thickness S must be much smaller than PZT and GGG thickness for best strain transfer and desired voltage induced uniaxial anisotropy. From available YIG films we chose the one with the lowest crystallographic uniaxial anisotropy field, H_{u1}^{G} = +8 Oe. In this situation, the effect of voltage-induced anisotropy should be the most distinct.

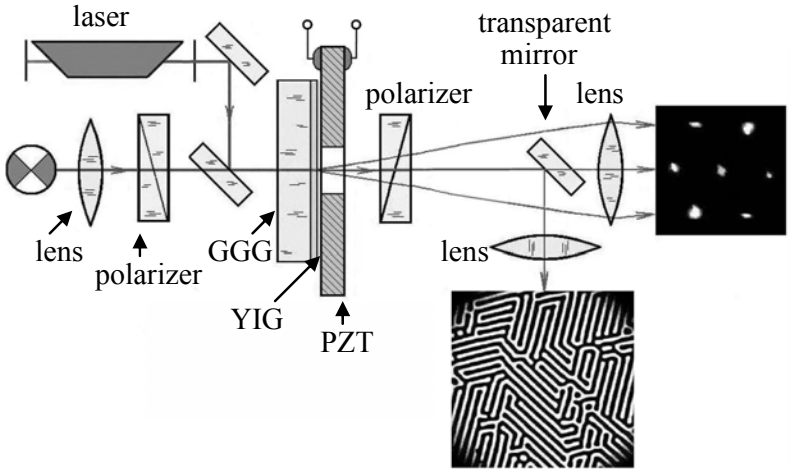

Fig.4. Schematic diagram showing the experimental set-up for magneto-optical measurements, imaging of domain structure, and diffraction pattern for YIG-PZT.

IV. Results and discussion

a. Voltage induced magnetization-flip phase transition

In the absence of any voltage or bias magnetic field applied to PZT, the YIG film showed irregular labyrinth domain structure as in Fig.5(a). When a magnetic field H_0 of several Oe was applied in the film plane parallel to [110], stripe domains lined up along [110] appeared as shown in Fig.5(b). Further increase in H_0 led to increase in width of energetically favorable domains, while total period changed only slightly as in Fig.5(c). Finally, for H_0 ($\geq H_{cub}$), the film reached magnetically saturated state.

It was found that a voltage applied to PZT can cause transitions involving flip of domain magnetization from perpendicular to canted structure or vise versa. If, for instance, the YIG film when subjected to $H_0 = 4$ Oe shows stripe domains with the out-of-plane magnetization as clearly seen in Fig.5(b). When a voltage $V_0 = 60$ V is applied across PZT the domain pattern deteriorates as in Fig 5(d) implying that the static magnetization in the domains is now inclined with respect to film plane. When the polarity of voltage is changed, domain structure remains the same, but the magnetic field required for reorientation of magnetization somewhat increased.

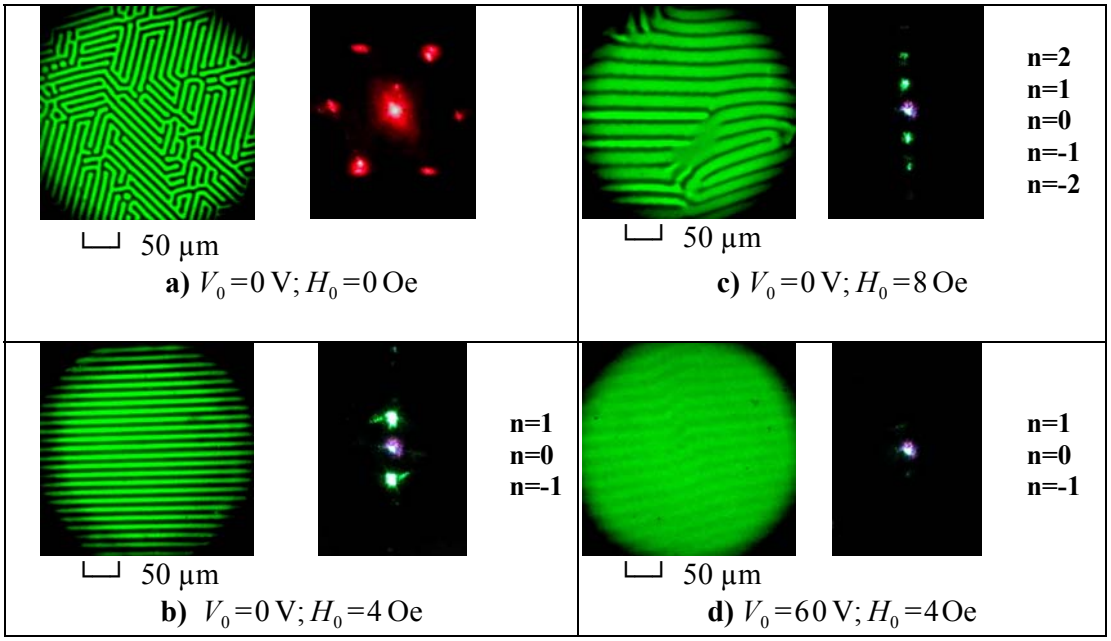

Fig. 5(a)-(c) Evolution of YIG domain structure and diffraction pattern under the influence of external magnetic field; (d) voltage-induced magnetization flip. n- denotes the diffraction order. The bias magnetic field is directed from left to right.

The domain structures in Fig.5 are as expected from the theoretical considerations in Section II. Indeed, the voltage applied to the PZT platelet causes a compressive or tensile stress (depending on the voltage polarity) which is transferred to the YIG via mechanically rigid bonding and creates stress-induced first-order uniaxial anisotropy field in accordance with Eq. (4). This field adds on to the uniaxial anisotropy field and, according to Eq.(1) and Fig. 2, results in modification of the equilibrium domain structure. It was found that for H_0=4Oe the magnetization-flip occurs for V_0 = 40 V. From Eq.(4), we calculated $H_{U1}^{E}(V)$ = -9.2 Oe, implying a total field $H_{U1}^{\Sigma} = H_{U1}^{G} + H_{U1}^{E}(V)$ = -1.2 Oe, that is rather close to theoretical value H_{U1}^{Σ} = -0.5 Oe (see Fig. 2). For larger magnitude of H_0 domains become unequal in width and the model is no longer valid and calculated values deviate from experiment.

b. Voltage modulation of transmitted light intensity

Further evidence for the electric-field induced magnetization-flip transition was obtained through studies on modulation of the intensity of light transmitted through the film. The YIG film with a periodic stripe domain structure is essentially a grating that formed a diffraction pattern showing interference maxima, located in the transverse direction (which is $[11\bar{2}]$ in our case) as shown in Fig. 5. The intensity of the first interference maximum is given by

$$I_1 = I_0 \frac{4}{\pi^2} \cdot \sin^2(\varphi_F \cdot M_z S) \cdot e^{-\alpha S} \qquad (5)$$

where I_0 is the intensity of a light beam entering the film, S is the thickness of YIG film, α=620cm^{-1} is the absorption coefficient at $\lambda = 628$ nm, and φ_F=$0.89 \cdot 10^{-3}$ deg/(μm G) is the angle of specific Faraday rotation in YIG. The relative intensity of the first maximum I_1/I_0 for YIG film is rather small, no more than 0.01% in the 633 nm and 0.02% in the 425 nm range. However, it is sufficient for direct observations and quantitative measurements. In YIG films doped with bismuth, diffraction efficiency rises and I_1/I_0 can reach 1% since the specific

Faraday rotation for pure bismuth iron garnet at a wavelength of 633 nm is two orders of magnitude larger than in pure YIG [30].

At first, we investigated the intensity of the first diffraction maximum as a function of DC bias voltage V_0 at $H_0 = 4$ Oe and the results are presented in Fig. 6 (after background signal subtraction). One can see a clear hysteresis in the intensity and $I_{max}/I_{min} \sim 10.5$ and modulation depth $(I_{max} - I_{min})/(I_{max} + I_{min})$ = 82%. The data is also another direct evidence of magnetization-flip transition; it implies that for large negative voltage the perpendicular component of magnetization in domains is appreciably smaller than at zero bias. Moreover, using Eq.(5) we can roughly estimate the magnitude of M_z in canted state. We estimate from the data that $M_z = 43$ G which is rather close to theoretical predictions (see Fig. 3).

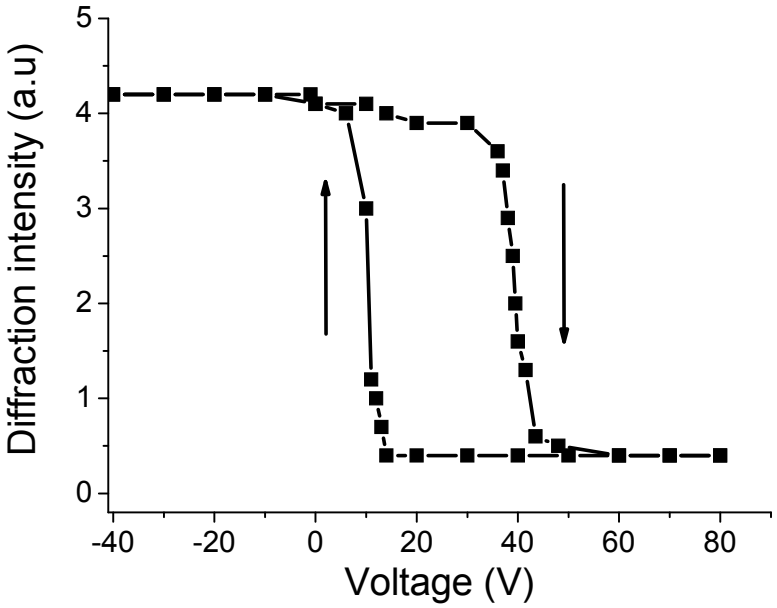

Fig. 6. Data showing the first order diffraction intensity maximum vs. voltage V for $H_0 = 4$ Oe.

There is qualitative agreement between the change in the diffracted intensity with bias voltage shown in Fig.6 and the anticipated electric field dependence of strain in PZT. The piezoelectric strain in PZT increases with increasing voltage, which in turn changes the magnetization direction and the domain structure. Far from the spin-flip region any change in the

magnetization direction is rather small, and the diffraction intensity does not show measurable dependence on the bias voltage. For voltages high enough to cause the spin-flip transition from one domain structure to another, the diffracted intensity changes abruptly. Theoretical estimates of the voltages using the strain-induced uniaxial anisotropy model are in agreement with the data.

In order to investigate the voltage induced magnetization-flip and the resulting modulation of light, we applied H_0 = 1 Oe and a DC voltage V_0 large enough to achieve a domain structure close to magnetization-flip point. Then we applied an ac voltage of meander shape and measured the time-dependent intensity of diffraction maxima and the data are presented on Fig. 7. One can see that sufficiently large voltage variation (peak-to-peak value V_{pp} was taken 16 V) leads to periodic rearrangement of the static magnetization in the domain structure, resulting in periodically varying intensity of the diffraction light. Indeed for the

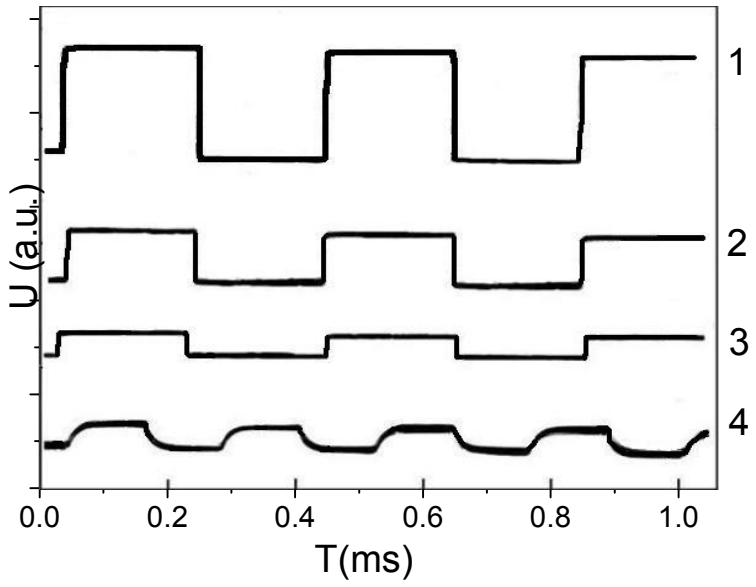

Fig. 7. Oscillograms of the diffraction intensity modulation by means of a.c. voltage, applied to PZT: 1 – V_0 =54 V, f=2.5 kHz; 2 - V_0 =64 V, f=2.5 kHz; 3 - V_0 =74 V, f=2.5 kHz; 4 - V_0 =54 V, f=4 kHz. Bias magnetic field H_0 = 1 Oe.

OOP magnetization case domains effectively act as a diffraction grating and diffraction maximum intensity is registered; for canted orientation the light passes through grating with much lower contrast (due to $\sin^2(\varphi_F \cdot M_z S)$ term in Eq. (5)) and the detector, placed in the position of first maximum, records much smaller signal. Fig. 7 shows the shape of output signal, which was almost identical to the shape of input one. Values of both the DC and pulsed voltages for light modulation can be drastically reduced if thinner piezoelectric layer could be used. For example, a 40 μm thick PZT will require 5 times smaller operating voltage.

Amplitude and shape of output signal remains steady for input signal frequencies *f* from 0 to 3 kHz. Further frequency increase leads to the progressive distortion and gradual decrease of modulation amplitude for *f* >3 kHz, that eventually fall down to almost zero at *f*=5 kHz. Figure 7 showing output signal measured at *f*=4 kHz illustrates this point and could be associated with acoustic modes in the sample as discussed below.

The radial acoustic mode frequency for the 10 mm diameter PZT used in this study is on the order of 6 kHz. Our experiments indicate substantial energy dissipation and sample heating when the modulation frequency is tuned to the resonance frequency. According to the data presented in Fig.7, for modulation frequencies above 4 kHz the shape of the intensity profiles become more and more distorted (Fig. 7. curve 4 for example) and the amplitude of modulation decreases until it the amplitude decreases to zero. It is quite possible, that such behavior is due to sample heating for frequencies close to the resonance frequency of whole PZT/YIG/GGG structure. Further studies are necessary to resolve this question.

Finally, it is also of interest to measure the M vs H for the composite under an electric field to confirm the magnetization flip observed by optical techniques in this study. The flip is expected to alter the shape of the M vs H loop upon the application of an electric field to PZT [6]. But our preliminary studies did not show any measurable variation in the M vs H

characteristics. Establishing a correlation between M vs H under an applied voltage and the domain structure in Fig.4 is a subject of interest for further investigation.

V. Conclusion

Electric field control of domain magnetization state has been studied in a bilayer of YIG and PZT. Both the domain observation by the Faraday effect and light diffraction measurements have been utilized to demonstrate the magnetization-flip to a canted state upon the application of a DC voltage across PZT. The resulting piezoelectric strain manifests as an uniaxial anisotropy field in YIG and leads to the spin-flip for a threshold voltage. The magnetization flip to the canted state is inferred from the change in the domain structure and the intensity of diffracted light. A theory that describes the magneto-optically observed magnetization-flip transition is presented. Theoretical estimates for the magnetization-flip voltage agree with experimentally measured values within the range of uncertainty due to ferroelectric hysteresis in PZT. The theory developed here is valid for any ferrite-piezoelectric composite for estimates on the respective magnetization state. The results presented here are of interest for electric field control of magneto-optical and spintronic devices.

Acknowledgments

The efforts at Oakland University were supported by a grant from the National Science Foundation (DMR-0902701).

References

[1] V. G. Bar'yakhtar, V. A. Borodin, V. D. Doroshev, N. M. Kovtun, R. Z. Levitin, E. P. Stefanovskii, Sov. Phys. JETP 47, 315 (1978).

[2] R. E. Bornfreund, D. C. Khan, P. E Wigen, M. Parvadi-Horvath, J.B. Ings, R.F Belt, J. Magn. Magn. Mater. 151, 181 (1995).

[3] A. V. Bezus, A. A. Leonov, Yu. A. Mamalui, Yu. A. Siryuk, Phys. Solid State 46, 283 (2004).

[4] C.-W. Nan, M.I. Bichurin, D. Viehland, S. Dong, G. Srinivasan, J. Appl. Phys. 103, 031101 (2008).

[5] M. A. Popov and I. V. Zavislyak, Tech. Phys. Lett. 38, 865 (2012).

[6] N. X. Sun and G. Srinivasan, SPIN 2, 1240004 (2012).

[7] C. Pettiford, S. Dasgupta, Jin Lou, S. D. Yoon, and N. X. Sun, IEEE Trans. Magn. 43, 3343 (2007).

[8] G. Srinivasan, A.S. Tatarenko, Y. K. Fetisov, V. Gheevarughese and M.I. Bichurin, MRS Proc. 966, 0966-T14-01 (2006).

[9] V. Petrov, G. Srinivasan, O.V. Ryabkov, S.V. Averkin, and M.I. Bichurin, Solid State Commun. 144, 50 (2007).

[10] F. Zavaliche, T. Zhao, H. Zheng, F. Straub, M. P. Cruz, P.-L. Yang, D. Hao, R. Ramesh, Nano Lett., 7, 1586 (2007).

[11] Tien-Kan Chung, S. Keller, G. P. Carman, Appl. Phys. Lett. 94, 132501 (2009).

[12] J. L. Hockel, A. Bur, T. Wu, K. P. Wetzlar, G. P. Carman, Appl. Phys. Lett. 100, 022401 (2012).

[13] T. Wu, A. Bur, P. Zhao, K. P. Mohanchandra, K. Wong, K. L. Wang, C. S. Lynch, G. P. Carman, Appl. Phys. Lett. 98, 012504 (2011).

[14] Chin-Jui Hsu, J. L. Hockel, and G. P. Carman, Appl. Phys. Lett. 100, 092902 (2012).

[15] I. V. Zavislyak and M. A. Popov, *Yttrium: Compounds, Production and Applications*, Ed. B. D. Volkerts (Nova Science Publishers, Inc., New York, 2011), p. 278.

[16] M. I. Bichurin and D. Viehland, *Magnetoelectricity in Composites* (Pan Stanford Publishing, 2011) p.286

[17] T. Aichele, A. Lorenz, R. Hergt, and P. Görnert, Cryst. Res. Technol. 38, 575 (2003)

[18] J. O. Artman, Phys. Rev., 105, 62 (1957).

[19] S. A. Kirov, A. I. Pilshchikov, and N. E. Syryev, Fiz. Tverd. Tela (Leningrad), 16, 3051 (1974).

[20] Yu. V. Gulyaev, P. E. Zil'berman, R. J. Elliott, and E. M. Epshtein, Phys. Solid State, 44, 1111 (2002).

[21] A. Hubert and R. Schäfer, *Magnetic Domains*, Springer-Verlag, Berlin (2009), p.686.

[22] T. E. Hasty, J. Appl. Phys, 35, 1434 (1964).

[23] H. Szymczak and N. Tsuya, Phys. Stat. sol. (a). 54, 117 (1979).

[24] M.A. Popov, I.V. Zavislyak, 22th Int. Crimean Conference on Microwave and Telecommunication Technology (CriMiCo'2012), pp. 593 - 594, 2012.

[25] A.B. Smith and R.V. Jones: J. Appl. Phys. 34, 1283 (1963).

[26] B. Hoekstra, F. van Doveren, and J. M. Robertson, Appl. Phys. 12, 261 (1977).

[27] M. Kubota, A. Tsukazaki, F. Kagawa, K. Shibuya,Y. Tokunaga, M. Kawasaki, and Y. Tokura, Applied Physics Express, 5, 103002 (2012).

[28] Yu. M. Yakovlev and S. Sh. Gendelev, *Ferrite monocrystals in radio electronics*, Soviet Radio, Moscow, 1975, 190 p. [in Russian].

[29] P. R. T. Pugh, J. G. Booth, J. W. Boyle, J.A. Cowen, A.D. Boardman, I. Zavislyak, V. Bobkov, and V. Romanyuk, J. Magn. Magn. Mater. 196-197, 498 (1999).

[30] T. Okuda, N. Koshizuka, K. Hayashi, H. Kobani, and H. Yamamoto, IEEE Trans. Magn. 5, 3491 (1987).